



بِسْمِ اللَّهِ الرَّحْمَنِ الرَّحِيمِ

Sudan University for Science and Technology
College of Petroleum Engineering and Technology
Department of Petroleum Exploration Engineering



Integrated Interpretation of Remote Sensing and Satellite Gravity – Atbara – Sudan

**تفسير متكامل لبيانات الإستشعار عن بعد و بيانات الجاذبية المقاسة بواسطة
الأقمار الإصطناعية – عطبرة – السودان**

Project Submitted in Partial Fulfillment of Requirement of the Degree
of B.Sc (Honor) in Petroleum Exploration Engineering

by:

- 1. Abualqurashi Mohamed Edris .**
- 2. Abobaker Hassan Edris .**
- 3. Mohamed Abdallah Dawood .**
- 4. Mohamed Omer Ali .**
- 5. Musab Ahmed Mohamed Ali .**

Supervisor:

Mr. Mohamed Salah Ahmed

October 2017

الإستهلال



قال تعالى :

(قَالُوا سُبْحَانَكَ لَا عِلْمَ لَنَا إِلَّا مَا عَلَّمْتَنَا إِنَّكَ أَنْتَ الْعَلِيمُ الْحَكِيمُ)

(البقرة 32)

صِدْقَةُ اللَّهِ الْعَظِيمِ

Dedication

Sudan University of science and technology

It's my second home where I belong.

I thank you for everything I learned inside you and what I've become.

Mother

She is precious in every way. The
source of kindness.

The sunshine's in my day.

The joy in my soul and the love of my life.

Father

He's a role model and a source of strength and inspiration.

He's the greatest man I've ever known and I'm so proud to be addressed
with him.

Brothers and sisters

They are ones who share me my childhood and stand beside me while no
one left aside.

My friends and classmates To
whom I appreciate.

To whom I love and care.

To whom I won't ever forget. To
whom I do respect.

Dear teachers

For your patience, caring, supporting and kind words sharing.

I just want to say thank you for everything along this period.

Acknowledgements

This research project would not have been possible without relief and the will of **Allah** and the support of many people, we would like to extend our deepest gratitude to our supervisor **Mr. Mohammed Salah** for giving us the opportunity to our research. We greatly indebted to his for his enduring confidence in us. We have learned many things from his rich academic and practical experience. His encouragement, support and patience always guided us throughout this period.

We are would also like to thank **Ms. Mai Alsadig** for providing us her time and acknowledge through teaching her wide practical experience in conducting software and how we can use it in our research project perfectly, and also **Mr. Azhari Abualgasim** for helping and supporting, and also we would like to thank everyone who extend a helping hand in the completion of this research project as well as members of **the Department of Exploration Engineering** .

Abstract

The study area lies in Northern Sudan and Situated In the River Nile State it is latitudes ($18^{\circ}0'13.75''$ - $16^{\circ}34'49.15''$ N) and longitudes ($32^{\circ}5'45.30''$ - $35^{\circ}29'59.64''$ E). 350 meters above sea level.

The main objective of the present study is to Identify the surface and subsurface structures in the study area and define the geometry of Atbara Basin. Different digital image processing techniques including spectral and spatial enhancement have been applied to Landsat 8 OLI image. The digital image processing of the remotely sensed data helped in the delineation of lineaments and drainage system in the study area.

Gravity point data obtained by satellite was used in the present study. Polynomial fitting was used in order to separate the regional from the residual component of the gravity. The first and second vertical derivatives and the first horizontal derivative were computed in order to study the presence of faults. Moreover, three profiles were constructed across the Bouguer anomaly map in an approximately, NE-SW directions cutting the most prominent anomalies in the area , then used to construct 2D gravity model.

The outcome of the present study is the modeling of the subsurface geology of the study area based on the Bouguer anomaly map and the above-mentioned three profiles.

الخلاصة

تقع منطقة الدراسة في شمال السودان و تتبع لولاية نهر النيل بين خطي عرض ($16^{\circ} 34'$ - $18^{\circ} 0' 13.75''$) و خطي طول ($32^{\circ} 5' 45.30''$ - $35^{\circ} 29' 59.64''$) شرقا ، على ارتفاع 350 متر فوق مستوى سطح البحر.

الهدف الاساسي من الدراسة هو تعيين التراكيب السطحية و تحت السطحية لمنطقة الدراسة و تحديد الشكل الهندسي لحوض عطبرة ، طبقت العديد من تقنيات معالجة الصور الرقمية بما فيها التعزيزات الطيفية و المكانية على صور (Landsat 8 OLI) ، معالجة الصور الرقمية للبيانات المستشعرة عن بعد ساعد في رسم التشققات و انظمة التصريف في منطقة الدراسة ، استخدمت في هذه الدراسة بيانات الجاذبية التي تم الحصول عليها عن طريق الاقمار الاصطناعية و تم استخدام طريقة مطابقة الحدود (polynomial fitting) لفصل الجاذبية الاقليمية عن الجاذبية المتبقية .

تم حساب المشتقة الرأسية الاولى ، المشتقة الرأسية الثانية و المشتقة الأفقية الاولى لتحديد مواقع الفوالق ، ثم عمل ثلاثة قطاعات على مناطق الشذوذ على طول خريطة الجاذبية قاطعةً حوض عطبرة الرسوبي ، ثم استخدمت لإنشاء نموذج ببع 2D .

مخرجات هذه الدراسة كانت عبارة عن نمذجة الجيولوجيا تحت السطحية لمنطقة الدراسة و تحديد سمك وعمق الرسوبيات فوق صخور الاساس .

List of Contents

Abstract.....	IV
الخلاصة	V
List of Contents	VI
List of Figures	VIII

Chapter One

Introduction.....	1
1.1. Location and Accessibility	1
1.2 Population.....	2
1.3. Topography.....	2
1.4. Climate and vegetation	3
1.5. Drainage	3
1.6. Problem statement	4
1.7. The Study Objectives:	4
1.8. Previous studies:	4

Chapter Two

Regional Geology & Tectonic Setting.....	6
2.1. Introduction:	6
2.2.1The Basement Complex	2.2.1.1. 7
The Basement Complex of Sabaloka.....	7
2.2.1.2. The Basement Complex in Bayuda Desert.....	7
2.2.1.3. The Basement Complex in Red Sea Hills.....	8
2.2.2. Nubian Sandstone Formation.....	8
2.2.3.Hudi Chert Formation	9

2.2.3. Superficial Deposits	10
-----------------------------------	----

Chapter Three

Literature Review	11
3.1 Remote Sensing.....	11
3.1.1 Remote Sensing Definition and History.....	11
3.1.2 Concepts of Remote Sensing.....	12
3.1.2.1 Electromagnetic Radiation (EMR).....	12
3.1.2.2 Electromagnetic Spectrum.....	12
3.1.2.3 Sensors.....	13
3.1.3 Landsat System.....	14
3.1.3.1 Landsat 8	14
3.1.3.2 Landsat 8 Bands	15
3.2 Geographic Information System (GIS)	16
3.3 Satellite Gravity	18
3.3.1 Satellite Altimetry.....	19
3.3.2 How Altimetry Works.....	20
3.3.3 Basics of Satellite Radar Altimetry.....	21
3.3.4. High-Precision Altimetry with Satellites Working Together.....	21
3.3.5 Altimetry Applications in geophysics.....	22
3.3.5.1 Bathymetry.....	23
3.3.5.2 Geodesy.....	23
3.3.6 Other Geophysical Applications.....	23

Chapter Four

Methodology.....	24
4.1 Remote sensing.....	24
4.1.1 Digital Image Processing	24
4.1.2 Pre Processing Technique	24

4.1.2.2 Radiometric Calibration	24
4.1.2.1 Flaash Atmospheric Correction	24
4.1.2.3 Mosaicking	25
4.1.2.4 Sub setting (Resize)	25
4.1.3 Processing Technique	26
4.1.3.1 Color Composite	26
4.1.3.2 Principle Component Analysis (PCA)	27
4.1.3.3 Extract Lineament Features.....	28
4.2 Gravity	29
4.2.1 Introduction	29
4.2.2 Bouguer Anomaly	29
4.2.3 Qualitative interpretation of Bouguer map.....	30
4.2.4 Regional – Residual Separation.....	31
4.2.5 First Vertical Derivative.....	33
4.2.6 First horizontal derivative.....	34
4.2.7 2DModeling.....	35
4.2.8 DensityMeasurement.....	36
4.2.9 Result and Discussion.....	36

Chapter Five

Conclusions and Recommendations.....	39
--------------------------------------	----

List of Figures Page

Fig (1.1): location of area study.....	1
Fig (1.2): Topographic map of the study area.....	2
Fig (1.3): Drainage system in the study area.....	3
Fig (3.1): Grounds tracks for the 4 operational satellites on June 2015.....	21
Fig (3.2): Altimeter sampling related to applications. Credits CLS.....	22
Fig (4.1): Subset of study area from Landsat image	25
Fig (4.2): color composite obtained using bands 7, 6, and1 in RGB respectively.....	26
Fig (4.3): Principle Component Analysis (PCA) using PC1, PC2 and PC3 in RGB.....	27
Fig (4.3): Extracted lineaments of the study area	28
Fig (4.4): Buoguer anomaly map of the study area.....	30

Fig (4.5): Residual gravity map of study area.....	33
Fig (4.6): First Vertical Derivative Map.....	34
Fig (4.7): First Horizontal Derivative Map.....	35
Fig (4.8): Gravity model of profile (1).....	37
Fig (4.9): Gravity model of profile (2).....	37
Fig (4.10): Gravity model of profile (3).....	38

Chapter one

Introduction

1.1. Location and Accessibility

The study area located in the northern Sudan in the River Nile state bounded by latitude $18^{\circ}0'13.75''$ north _ $16^{\circ}34'49.15''$ north and longitude : $32^{\circ}5'45.30''$ east _ $35^{\circ}29'59.64''$ east , 350 meters above sea level. It is located 10 kilometers of the city of Damar, The distance from Khartoum to the study area is about 200 Km, and can be reached from Khartoum by a high way passing through Shendi Town, to Atbara, following the River Nile on the eastern bank. The Sudan railway line at the right bank of the Nile joining Khartoum – Atbara, can also be used to reach the area.

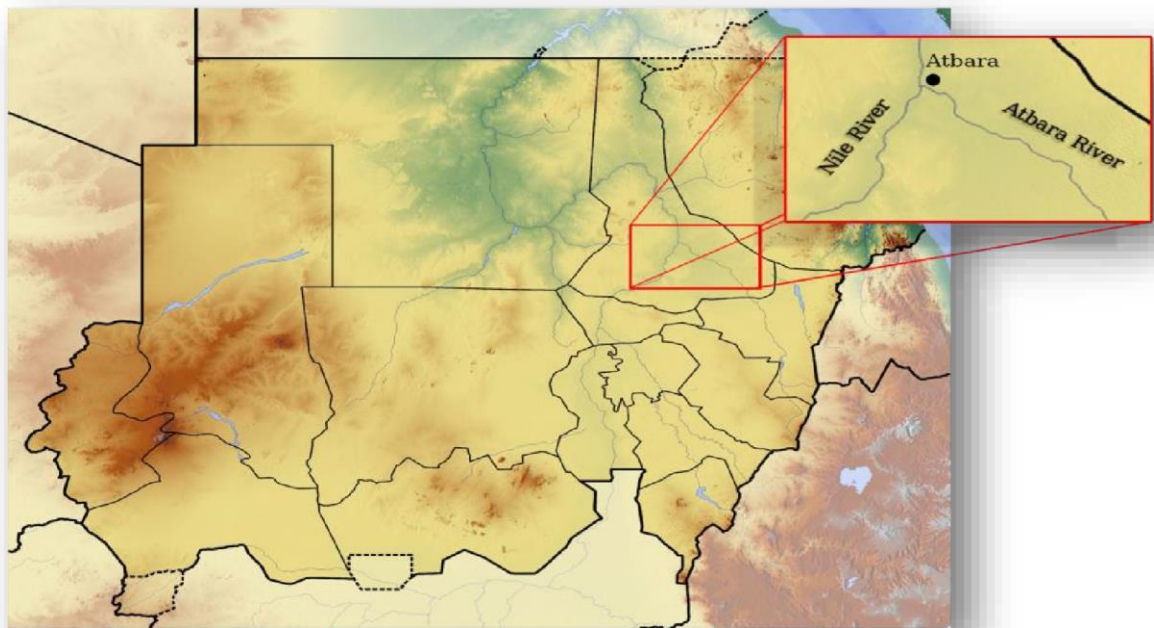


Fig (1.1): showing location of area study

1.2. Population

The population of area is a mixture of a number of Sudanese races, and they have brought this city to work and earn a living .the economic situation of most residents of Atbara is simple for the annual period. The city of Atbara is a city closer to the industrial than agricultural.

1.3. Topography

Topographically, the area is characterized by low to medium relief, mountains and some of low relief features valleys and plains. It is gently sloping from the east to the west and from the south to the north. There is high land at Jebel Umm Ali, and low land at the River Atbara junction with the River Nile.

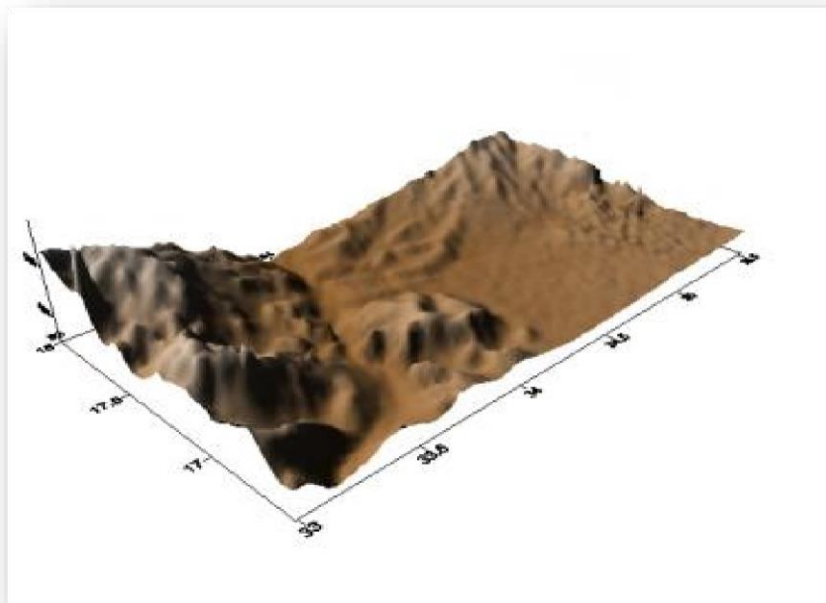


Fig (1.2) Topographic map of the study area

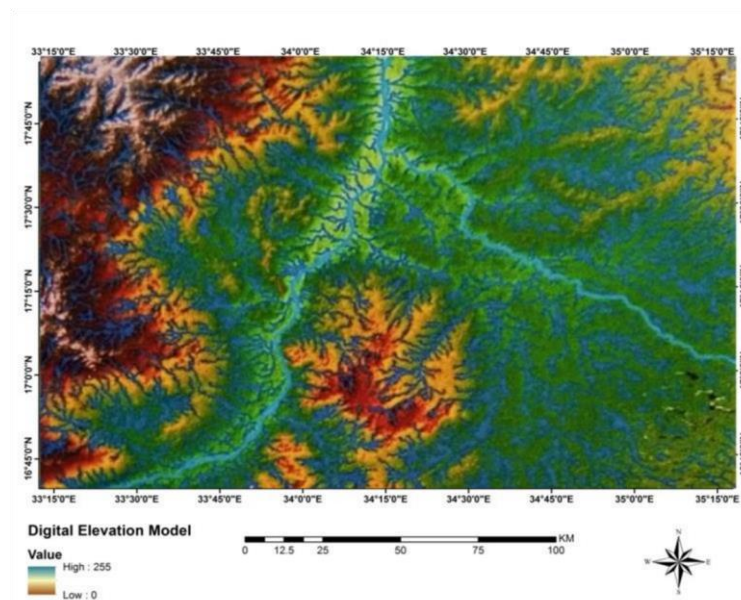
1.4. Climate and Vegetation

The area is dominated by arid climate conditions with a hot summer season extending from March to August with temperature reaching above 45°C during the day. The average temperature is about 35°C. The rainy season is extending from July to September with less than 200 mm per year rainfall. The winter season is from November to February and the temperature drops to less than 20°C.

Generally, the area is poor in vegetation. The vegetation cover includes Acacia trees and short grasses along the seasonal valleys. There are date palm trees along the River Nile in addition to some other crops grown in the terraces of the River Nile.

1.5. Drainage

The area is dominated by parallel to sub dendritic seasonal streams flow in sedimentary rocks and seems to be structurally controlled. The main direction of these streams is to the W and NW, towards the River Nile (Fig. 1.3).



Fig(1.3) Map showing the drainage system in the study area

1.6. Problem Statement

Atbara basin is the most important interior northern Sudan Mesozoic-Cenozoic rift basins, the geometry of the basin and structural elements was not studied enough, in the research we will use latest available technologies of remote sensing and satellite gravity to better understand the surface and subsurface image of the sedimentary basin and structural features.

1.7. The Study Objectives

The study aims mainly to give a detailed description of the geology and structures of the study area basin using available data from remote sensing and satellite gravity, combined in geographic information systems (GIS) platform. And further specifically:

- 1) Identification of the surface and subsurface structures in the study area.
- 2) Definition of the geometry of Atbara Basin.

1.8. Previous Studies

Jorgensen and Bosworth (1989): Made gravity modeling in the Central African Rift System, Sudan, and identified rift geometries and tectonic significance.

Bussert (1993): Studied the intracratonic basins evolution in the central northern Sudan showing the contrast with typical cratonic sandstone sheets of North Africa.

Salama (1997): Studied the Sudanese intracratonic rift basins on the basis of geophysical survey, delineating NW-SE trending Cretaceous sediment troughs and mentioned that wadi El Mukabrab in the northern part of the study area represents a fault boundary.

Ahmed and Badi (2008): Conducted research to detect the bacteriological pollution of groundwater in Shendi-Atbara Basin, River Nile State, Sudan. He found in Atbara Area that basement is shallow and the sandstone rocks possess high porosity which enhance the downward infiltration, beside the absence of thick layers of mudstones to separate the upper zone from the lower ones. Groundwater pollution was reported overall area of settlements. E.Coli is present in the groundwater as an indication of groundwater pollution; some polluted wells are also chlorinated.

Omer (2013): Studied groundwater sources, geological formations, and their environment in Sudan.

Chapter Two

Regional Geology & Tectonic Setting

2.1. Introduction

Atbara Basin is one of the interior Sudan Mesozoic-Cenozoic rift basins located in the north-central of Sudan with stratigraphic sequences of Jurassic to Cretaceous with mainly fluvial and lacustrine deposits. Stratigraphically the basin sedimentary succession is made up of the Bagrawiya, Mahmiya and Shendi Formations. The Mahmiya Formation is the main source rock in the basin with the reservoir and cap rocks both in the Shendi Formation. The geological and geophysical studies in the Atbara Basin have shed light on the geology and tectonic settings of the basin.

The sedimentary succession of the Atbara Basin forms an outlier in relation to the surrounding Precambrian crystalline rocks which crop out in Sabaloka inlier, Butana plain and Bayuda Desert.

As with the case of most Sudanese interior rifts, Atbara Basin is related to the Central African Shear Zone. Modeled gravity data shows half graben geometry with the major bounding fault lying on the northeastern side of the basin, which correspond well with the course of the Atbara River.

Regionally the chronological arrangements of the stratigraphic units in the area have been conducted as follows:

4- Superficial Deposits.

3- Hudichert Formation.

2- Nubian Sandstone Formation.

1- Basement Complex.

2.2.1. The Basement Complex

The formations is an outlier surrounding by the pre-Cambrian and Paleozoic crystalline rocks, and the basin bounded from south by the sabaloka basement complex, butana plain extended to the south and east. Bayuda desert to the westsouthwest.And the Red Sea hills to the North east.

2.2.1.1. The Basement Complex of Sabaloka Area

Dominated by grey gneisse with patches of granulite of pan-African age (Dawoud and sadig,1988) it was later intruded by poorly foliated granitic rocks and post orogenic younger granites, including the ring complexes(Almond1971,1977).

2.2.1.2. The Basement Complex in Bayuda Desert

Represented by The Neoproterozoic crust of the Nubian Shield which related to the Pan-African Orogeny (950-550 Ma). (Kennedy, 1964; Greenwood et. al, 1976). Rock associations of dismembered Arc volcanics and associated intrusive granitic rocks, immature sediments and ophiolites of arc and back arc basin affinities dominate it, which are predominantly in the Greenschist facies of metamorphism. The western part of Bayuda Desert is dominated by low-grade assemblage of the Nubian Shield to the east. Based on field and petro-graphical evidence, structural Relationships, and in the absence of radiometric dating. Vail (1979) classified the Precambrian rocks of the Bayuda Desert into three groups separated by unconformities

- (1) Older group of gneisses (Grey gneisses).
- (2) Amphibolite facies metasediments.
- (3) Upper group of volcanoclastic rocks (the greenschist assemblage).

2.2.1.3. The Basement Complex in Red Sea Hills

Region of NE Sudan is part of the Arabian-Nubian Shield of Proterozoic era. It lies in the central part of the Nubian segment. It extends northwards through the eastern desert of Egypt and Southwards across the Sudan-Eritrean border into the Ethiopian plateau. To the east is bound by the By the Red Sea coastal plain and the Nubian Desert to the west.

Several geologists (Gass, 1955; Ruxton 1956; Gabert et.al. 1960; Kabesh, 1962; Ali, 1979; Vail, 1979, 1982; El Nadi, 1984) have described the geology of the Red Sea Hills of NE Sudan.

2.2.2. Nubian Sandstone Formation

This is to designate siliceous conglomeratic sandstone with substantial clays of upper cretaceous age and recommended that the term of (NST) should commonly use to describe a facies and therefore has no stratigraphic value.

Subsequently the term ‘Nubian series’ has been abounded for the incorrect use of the term ‘series’ which has chronostratigraphic value and should not be used in lithostratigraphic sense (Whitman, 1971

In Sudan Kheiralla (1966) and Whitman (1971) used the term ‘Nubian sandstone’ to designate the sediments in details along the Nile and reported that these sediments occupied about 25.7% of the area of the Sudan extending from south Egypt into Kordofan parallel to the River Nile. Of variegated color lying unconformable on the Precambrian basement and Paleozoic formation (Whitman, 1965). comprising from conglomerate, sandstone, sandy mudstones, mudstone and underlying unconformable by Hudi Chert, and Quaternary sediments.

The term Nubian Sandstone applies to the Paleozoic and Mesozoic sandstone occurring in the Nubian Desert of Egypt (Rüssegger, 1837), Libya and Sudan, and early reported by Sanford (1935) for north-western Sudan.

The Nubian sandstone is mainly composed of lenticular basal conglomerate followed by immature quartzitic sandstone topped by thin shale crust. It is characterized by cross-bedded structure with localized horizontal bedding and most common horizontal type of bounding surface overlying the basement and upper Cretaceous

The Nubian Sandstone Formation is mainly composed of conglomerates, sandstones, sandy mudstones and mudstones which rest unconformably with the Basement Complex.

2.2.3. Hudi Chert Formation

The Hudi chert was first identified by Cox (1932) from Hudi Railway Station about 40 km NE of Atbara and later studied by Andrew and Karkains (1945), Andrew (1948), Whiteman (1971) and Barth and Meienhold (1979).

The Hudi chert rocks were regarded as lacustrine chalky deposits that have been silicified into chert (Andrew and Karkains, 1945). The source of silica was probably from silica flow from the young volcanic activity of Jebel Umm-Marafieb of NW Berber. Cox (1932) reported that the Hudi chert is an upper Eocene/lower Oligocene Formation, which contains some types of fossils such as Gastropods and plant fossils.

In this study, cherts have been found in the NE of Atbara in the flat plain underlain by the deformed Cretaceous sediments.

2.2.3. Superficial Deposits

All the lithology mentioned above are covered by Quaternary to Recent sediments. These sediments include gravels, sands, clays, sandy clays and silt. The alluvial deposits are very thick around the River banks consisting mainly of dark clays and clayey silt with fined-grained sands used for Cultivation.

The Wadi alluvial consists of fined to medium-grained sands, which form the middle and lower courses of the Wades, while the upper parts are covered with unconsolidated coarse sand and fine gravels.

Chapter Three

Literature Review

3.1. Remote Sensing

3.1.1. Remote Sensing Definition and History

Remote Sensing is the art and science of acquiring information about the earth surface without having any physical contact with it. This is done by sensing and recording of reflected and emitted energy. (Robert schowengerdt, (2007))

The modern discipline of remote sensing arose with the development of flight. The balloonist (G. Tournachon alias Nadar) made photographs of Paris from his balloon in 1858. Messenger pigeons, kites, rockets and unmanned balloons were also used for early images. With the exception of balloons, these first, individual images were not particularly useful for map making or for scientific purposes.

The development of artificial satellites in the latter half of the 20th century allowed remote sensing to progress to a global scale as of the end of the Cold War. Instrumentation aboard various Earth observing and weather satellites such as Landsat, the Nimbus and more recent missions such as RADARSAT and UARS provided global measurements of various data for civil, research, and military purposes. Space probes to other planets have also provided the opportunity to conduct remote sensing studies in extraterrestrial environments

Recent developments include, beginning in the 1960s and 1970s with the development of image processing of satellite imagery. Several research groups in Silicon Valley including

NASA Ames Research Center, GTE, and ESL Inc. developed Fourier transform techniques leading to the first notable enhancement of imagery data. (Citation needed) In 1999 the first commercial satellite (IKONOS) collecting very high resolution imagery.

3.1.2. Concepts of Remote Sensing

3.1.2.1. Electromagnetic Radiation (EMR)

The most important component of Remote Sensing is the Energy source to illuminate the Target. The energy is in the form of Electromagnetic Radiation. It is either natural originating from the Sun or earth by emission, or by artificial means. Electromagnetic energy refers to all the energy that moves with the velocity of light in a harmonic wave pattern. EMR consists of an Electrical field and Magnetic field. The electrical field varies magnitude in a direction perpendicular to the direction in which the radiation is travelling and magnetic field oriented to the right angles to the electrical field.

3.1.2.2. Electromagnetic Spectrum

The Electromagnetic Spectrum ranges from kilometers to nanometers. These are divided by ranges called Spectral bands. There are several regions in the Electromagnetic spectrum which is useful for Remote Sensing

3.1.2.3. Sensors

Remote sensor are the instrument which detect various objects on the earth's surface by measuring electromagnetic energy reflected or emitted from them; there are two types of remote sensing sensor

A. Passive Sensors

The passive sensors measure reflected sunlight that was emitted from the sun. Passive sensors measure this natural energy at specific frequencies (ν) (i.e. wavelength λ). For example, sensors can measure visible (390-700 nm), infrared (750 nm – 1 mm), ultraviolet (100-400 nm) and more types of EM radiation. These wavelength ranges are known as “bands”.



Sensors can have multiple bands (3 to 10 bands) known as “multispectral” imaging. Hundreds of finer bands is known as “hyperspectral” imaging.

Passive sensors would miss the sun if it disappeared because it measures natural energy being reflected at specific frequencies

B. Active sensors

The passive sensors have its own source of light or illumination and its sensor measures reflected energy. There are many advantages of Active Sensors summarized below:

- An advantage of active sensors is that they can be used at any time of the day because it does not require natural light. Active sensors can also produce microwave energy. This is advantageous because microwaves are generally not affected by any type of cloud cover.

- Two of the key advantages of active remote sensing are being able to collect imagery night and day, as well as through clouds and various weather conditions.

3.1.3. Landsat System

The Landsat Program is a series of Earth-observing satellite missions jointly managed by NASA and the U.S. Geological Survey. The program aimed at gathering facts about the natural resources of the Earth from earth-observing satellites carrying sophisticated remote sensing observation instruments.

In cooperation with NASA, on July 23, 1972, the Earth Resources Technology Satellite (ERTS-1) was launched. It was later renamed Landsat 1. Additional

Landsat satellites followed in the 1970's and 1980's, and in 1999, Landsat 7 was launched. Landsat 8 (initially named Landsat Data Continuity Mission - LDCM) was the most recent satellite to be launched on February 2013. Landsat 9 is in development, with a launch scheduled for late 2020.

The instruments aboard the Landsat satellites have acquired millions of images through the course of the missions, and the data are a valuable resource for global change research and applications in agriculture, forestry, geology, regional planning, and education.

3.1.3.1. Landsat 8

The Landsat 8 satellite images the entire Earth every 16 days in an 8-day offset from Landsat 7. Data collected by the instruments onboard the satellite are available to download at no charge from Earth Explorer, GloVis, or the Landsat Look Viewer within 24 hours of acquisition.

The spectral bands of the OLI sensor provides enhancement from prior Landsat instruments, with the addition of two additional spectral bands: a deep blue visible channel (band 1) specifically designed for water resources and coastal zone investigation, and a new shortwave infrared channel (band 9) for the detection of cirrus clouds.

The TIRS instrument collects two spectral bands for the wavelength covered by a single band on the previous TM and ETM+ sensors. Descriptions of the band designations for all Landsat sensors, and information about the comparisons between Landsat 8 and previous bands are also available.

These sensors both provide improved signal-to-noise (SNR) radiometric performance quantized over a 12-bit dynamic range. (This translates into 4096 potential grey levels in an image compared with only 256 grey levels in previous 8-bit instruments.) Improved signal to noise performance enable better characterization of land cover state and condition. Products are delivered as 16-bit images (scaled to 55,000 grey levels).

A Quality Assessment band is also included with each Landsat 8 data product. This band allows users to apply per pixel filters to the Landsat 8 Operational Land Imager (OLI)-only and Landsat 8 OLI/Thermal Infrared Sensor (OLI/TIRS)combined data products.

3.1.3.2. Landsat 8 Bands

Landsat 8 measures different ranges of frequencies along the electromagnetic spectrum a color, although not necessarily a color visible to the human eye. Each range is called a band, and Landsat 8 has 11 bands.

Landsat numbers its red, green, and blue sensors as 4, 3, and 2, so when we combine them we get a true-color image

Operational Land Imager (OLI)

Table (3.1) showing OLI spectral Bands

Band Name	Bandwidth (µm)	Resolution (m)
Band 1 Coastal	0.43 - 0.45	30
Band 2 Blue	0.45 - 0.51	30
Band 3 Green	0.53 - 0.59	30
Band 4 Red	0.63 - 0.67	30
Band 5 NIR	0.85 - 0.88	30
Band 6 SWIR 1	1.57 - 1.65	30
Band 7 SWIR 2	2.11 - 2.29	30
Band 8 Pan	0.50 - 0.68	15
Band 9 Cirrus	1.36 - 1.38	30

3.2. Geographic Information System (GIS)

Geographic Information Systems (GIS) can be defined as a computer-based systems that enable users to collect, store, process, analyze, modeling, display/output and present spatial data. (Trisurt, 2002)

It provides an electronic representation of information, called spatial data, about the Earth's natural and man-made features. A GIS references these real-world spatial data elements to a coordinate system. These features can be separated into different layers. A GIS system stores each category of information in a separate "layer" for ease of maintenance, analysis, and visualization.

The development of GIS is the result linking parallel developments of several other spatial data processing disciplines such as cartography, computer aided design, remote sensing technology, surveying and photogrammetry.

GIS software acts as an interface, or window, for viewing and manipulating GIS data. Each GIS file is georeferenced, meaning that the file is actually tied and related to real locations on the earth. GIS file has also been created based on a particular projection and coordinate system which means that files that share the same reference systems can be laid on top of each other. Since projections and coordinate systems are highly standardized, GIS data can easily be shared. The basic data types in a GIS reflect traditional data found on a map. Accordingly, GIS technology utilizes two basic types of data:

- * Spatial data: describes the absolute and relative location of geographic features.
- * Attribute data: describes characteristics of the spatial features. These characteristics can be quantitative and/or qualitative in nature. Attribute data is often referred to as tabular data.

The files stored in several formats, and each format comes in several different file types. Major formats and file include:

- Raster; represent a continuous surface that is divided into grid cells of equal size. Each cell appears as a particular color based on some value (i.e. reflected light). Files in the raster format are similar to digital photos. Common raster objects include air photos, Satellite imagery, and paper maps that have been scanned. There are many different file formats, some common ones include Tiffs (.tif), (.JPEGs) (.jpg), and S1D (.sid). Unlike regular tif or .jpg files, GIS raster files are georeferenced.
- Vector; consists of discrete coordinates and surfaces that are represented as individual points, lines, or polygons. Vector files appear to be more “maplike” and are always abstractions rather than actual images (i.e. shapes to represent boundaries points to represent cities). Common file formats are ESRI

shapefiles (.shp) ESRI coverages (.cov), Google KMLfiles (.kml) and GRASS vector files.

- Tables; data tables that contain records for places can be converted to GIS files and mapped in several ways. If the data contains coordinates like latitude and longitude, the data can be plotted and converted to a vector file. If each data record contains unique ID codes for each place, those records can be joined to their corresponding features in a GIS file and mapped, Tables are commonly stored in text files like .txt or .csv, database files like .dbt. Or in spreadsheets like Excel.
- Geodatabases; containers that can hold related raster, vector, and tabular data in one place. They are good for consolidating and organizing data. Geodatabases can be desktop (Microsoft Access .mdb, ESRI file geodatabases .gdb, Spatialite files .sqlite) or server based (PostGIS.

ArcSDE).

Today, GIS is considered as an important tool in planning and decision-making. It has been applied in many fields, such as cadastral mapping, land use planning, forestry, wildlife management, infrastructure planning, zoning, military, environmental monitoring, network planning, facility selecting, including socioeconomic applications. Some of the advanced applications at present involve air traffic monitoring, road navigation, crime analysis and so on.

3.3 Satellite Gravity

Satellite gravity derived from satellite altimetry, to free air gravity is not new. In the early 1980s William Haxby (Lamont Doherty Geological Observatory) produced the first global marine gravity map from SeaSat satellite altimeter data using interorbital track spacing of about 180 km. Haxby's map had a significant

impact on plate tectonic theory because marine free-air gravity data were able for the first time to uniformly image the tectonic fabric of the earth's oceanic crust. Since that time, much effort has been applied to improving satellite-derived gravity resolution. A major advance occurred in 1995, when the altimeter data from Geodetic Missions (GM) of GeoSat and ERS-1 satellites were released.

3.3.1 Satellite Altimetry

Altimetry is a technique for measuring height. Satellite altimetry measures the time taken by a radar pulse to travel from the satellite antenna to the surface and back to the satellite receiver. Combined with precise satellite location data, altimetry measurements yield sea-surface heights.

People have long been mystified by the oceans, long felt powerless when sailing them. The arrival of satellite-based systems, offering location, data collection and remote sensing, gave scientists a chance to think globally. Instruments were flown on missions to measure temperature, chlorophyll concentrations and surface wind velocity. But the real breakthrough in ocean observation was satellite radar altimetry

Global observation for a better understanding of oceanic phenomena is a reality: the ocean's role in past and future climate change is now a fact. And tomorrow, thanks to the continuing efforts to access altimetry data in near-real time and the improvement of technology, the progress of operational oceanography will bring close the coast.

In 1849, Matthew Maury published the first worldwide wind and current maps from data gathered by ships. The first purely oceanographic experiment was conducted in 1872: for 42 months, the Challenger expedition systematically

explored the oceans, collecting data from the sea surface down to the seafloor, such as bathymetry (depth soundings), temperature and current data. This information laid the foundations for modern oceanography.

At a global scale, in 1957, the Earth is an unknown planet. The creation of the International Geophysical Year (AGI) in 1957-1958 will fill this gap. Its goal was to measure the parameters (such as the Earth's hemispheric asymmetry) to get a first overview of some basic phenomena.

1957 is also the year of the first artificial satellite which we have just celebrated the fiftieth anniversary. Beyond the political strategies during its launch, Sputnik showed a new exploration way: the space.

An initial exploration phase begins in the 60's when geodetic satellites measure the first orbit calculated from distance measurements by laser telemetry. This calculation of orbital trajectory parameters will soon be doubled with the use of the Doppler shift.

3.3.2. How Altimetry Works

Altimetry satellites basically determine the distance from the satellite to a target surface by measuring the satellite-to-surface round-trip time of a radar pulse. However, this is not the only measurement made in the process, and a lot of other information can be extracted from altimetry. The magnitude and shape of the echoes (waveforms) also contain information about the characteristics of the surface which caused the reflection. The best results are obtained over the ocean, which is spatially homogeneous, and has a surface which conforms to known statistics. Surfaces which

are not homogeneous, which contain discontinuities or significant slopes, such as some ice, rivers or land surfaces, make accurate interpretation more difficult.

3.3.3. Basics of Satellite Radar Altimetry

- Exploring the Ocean Basins with Satellite Radar Altimetry (SIO)
- Radar Altimetry Tutorial (CLS / CNES / NASA)
- Satellite Altimetry Applications: Geodesy and Geophysics (AVISO+)
- Ocean Bathymetry and Plate Tectonics (SIO)

3.3.4. High-Precision Altimetry with Satellites Working Together

In many ways, the orbit of an altimetry satellite is a compromise. But one point that deserves special attention is getting the right balance between spatial and temporal resolution: a satellite that revisits the same spot frequently covers fewer points than a satellite with a longer orbital cycle. One solution is to operate several satellites together.

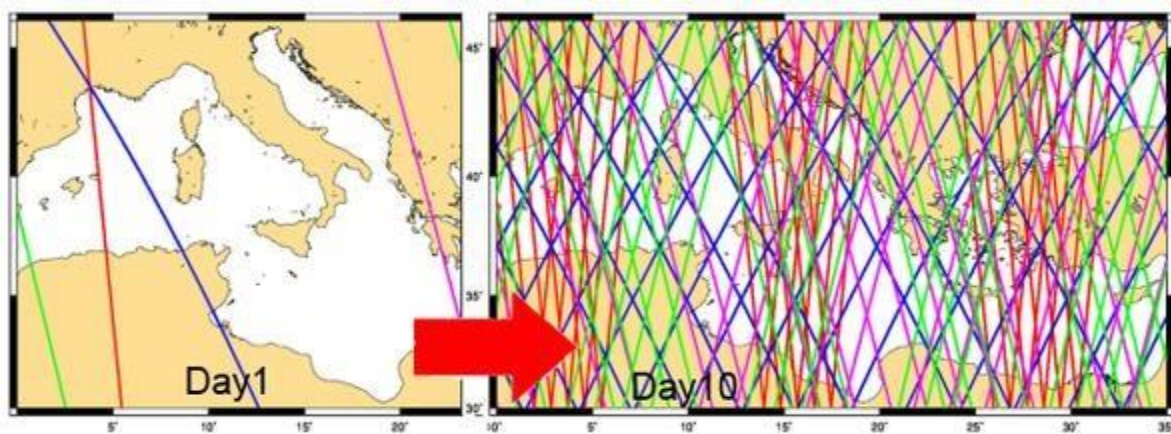


Fig (3.1) Grounds tracks for the 4 operational satellites on June 2015 .

At least two altimetry satellites are required to map the ocean and monitor its movements precisely, particularly at scales of 100 to 300 kilometres (mesoscale). With four altimetry satellites available (Jason-1+Jason-2+Envisat+Cryosat-2 from 2012, or Jason-1, Envisat or ERS-2, Topex/Poseidon and GFO between 2002-2005), the resolution of sea surface height measurements is greatly enhanced. At least three satellites are needed to observe eddies and mesoscale phenomenon.

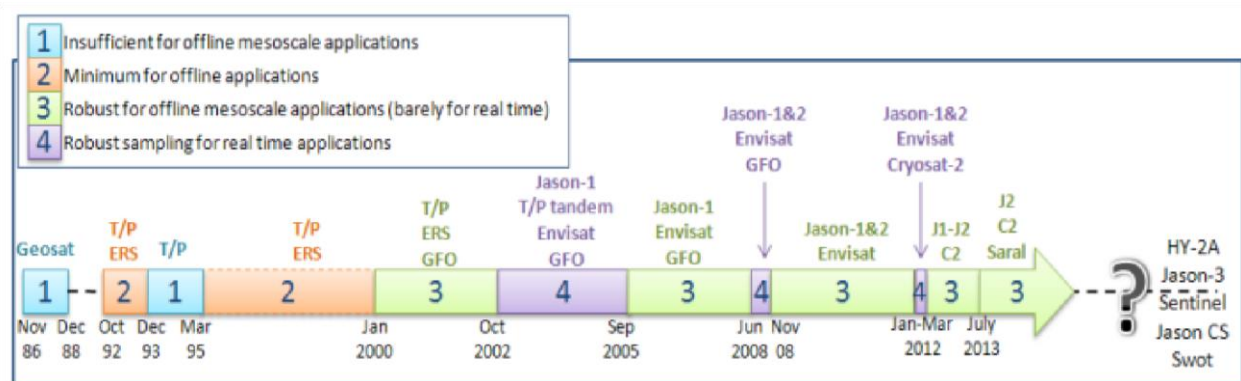


Fig (3.2) Altimeter sampling related to applications. Credits CLS.

3.3.5. Altimetry Applications in geophysics

Altimetry became an essential contribution to be used to study the Earth's shape and size, gravity anomalies (geodesy), seafloor relief (bathymetry), tectonic plate motion and rifts (geophysics), etc. Although often linked to plate tectonics, tsunamis are very different, transient phenomena. However, their impact on the sea surface can be seen by altimeters in some cases, thus helping the study of their propagation.

3.3.5.1. Bathymetry

Dense satellite altimeter measurements can be used in combination with sparse measurements of seafloor depth to construct a uniform resolution map of the seafloor topography.

3.3.5.2. Geodesy

Geodesy is the science of the Earth's shape and size. Altimetry makes it possible to compute Mean Sea Surface; such a surface includes the geoid, i.e. the shape of the sea surface, assuming a complete absence of any perturbing forces (tides, winds, currents, etc.).

3.3.6. Other Geophysical Applications

Altimetry also makes it possible to start on other geophysical applications; tectonic plate motions, poles motions, crustal motions, International Reference System, Earth's Centre of gravity... Doris, precise orbit determination and positioning onboard altimetry satellites, becomes a real space surveyor to develop geodesy and geophysics applications.

Chapter four

Methodology

4.1 Remote Sensing

4.1.1 Digital Image Processing

Digital image processing is the manipulation of digital data by computer programs in order to improve the appearance of an image (Gibson, 2000).

4.1.2 Pre Processing Technique

4.1.2.1 Radiometric Calibration :

Radiometric Calibration provides options to calibrate imagery to radiance, reflectance, or brightness temperatures. Radiometric Calibration for more information on how each option is computed.

The available calibration options depend on what metadata is included with the imagery. Most vendors distribute a metadata file or ephemeris data along with the image data.

4.1.2.2 FLAASH Atmospheric Correction

Solar radiation from the Sun emits scattering within the atmosphere, and atmospheric scattering is greater on light rays with shorter wavelengths, as in Land sat. These scattered rays are added to the radiation reflected from the Earth's surface to the spacecraft, thereby reducing the degree of variation within the space image. This correction is intended to modify the intensity of the light by deleting the value of the radiated radiation from the values of the image elements.

4.1.2.3 Mosaicking

The regional coverage of individual Landsat images can be extended by adjacent images into a mosaic which required uniform scale and minimum Distortions before combination. If the images pertain in different seasons or time, the mosaic will give sharp radiometric boundary between images.

This process included the collection of 3 satellite images of the study area after they were configured in the first phase. By applying this method, the full scene of the study area was obtained. This process resulted in a unified image showing the Atbara basin.

4.1.2.4 Sub setting (Resize)

Spatial sub setting was performed on the raw digital images including bend I 2, 5. 6. 7 & 8 in order to resize the image to the following coordinates Latitude $18^{\circ} 0' 13.75''$ N_ $16^{\circ} 34' 49.15''$ N and longitude $32^{\circ} 5' 45.30''$ E_ $35^{\circ} 29' 59.64''$ E.

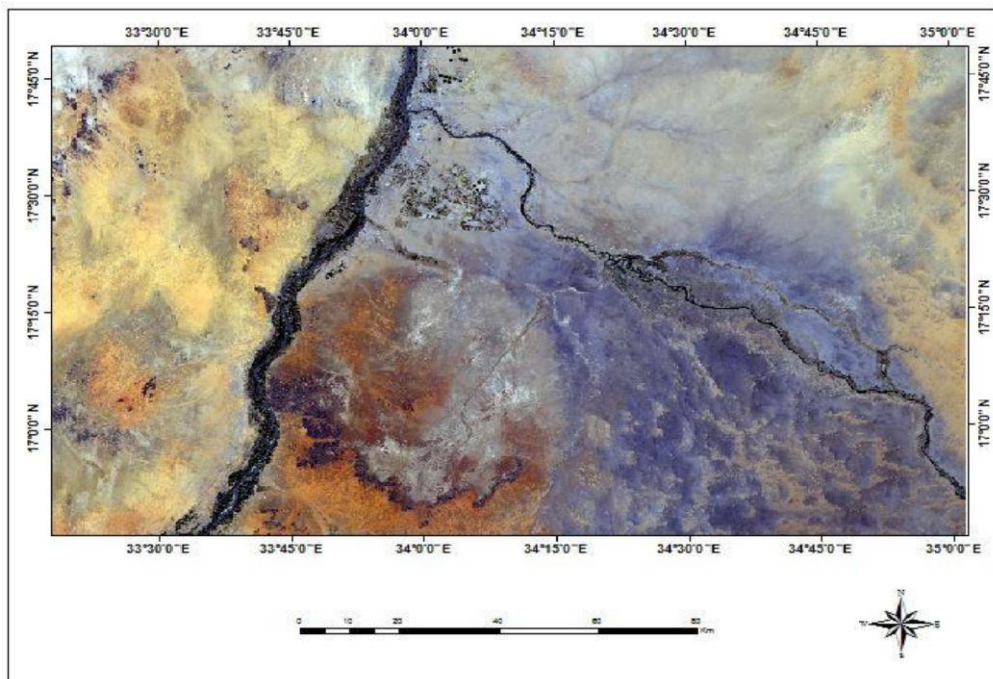


Fig (4.1): subset of study area from Landsat image

4.1.3 Processing Technique

4.1.3.1 Color Composite

A colored image made by assigning red, green, and blue colors to each of the separate monochrome bands of a multispectral image and then superimposing them. A color composite gives a visual impression of 3 raster bands. Putting the three bands together in one color map can give a better visual impression of the reality on the ground, than by displaying one band at a time. Examples of color composites are false color (or IR) images and ‘natural color’ images. The input pixel values of each band are measures of the amount of reflection in a certain wavelength interval. The values in the output color composite map just refer to certain colors. By using bands 7,6,1 and we were found best band combinations in identifying liner patterns of geological formation boundaries, river channels and vegetation which shown in fig (4.2)

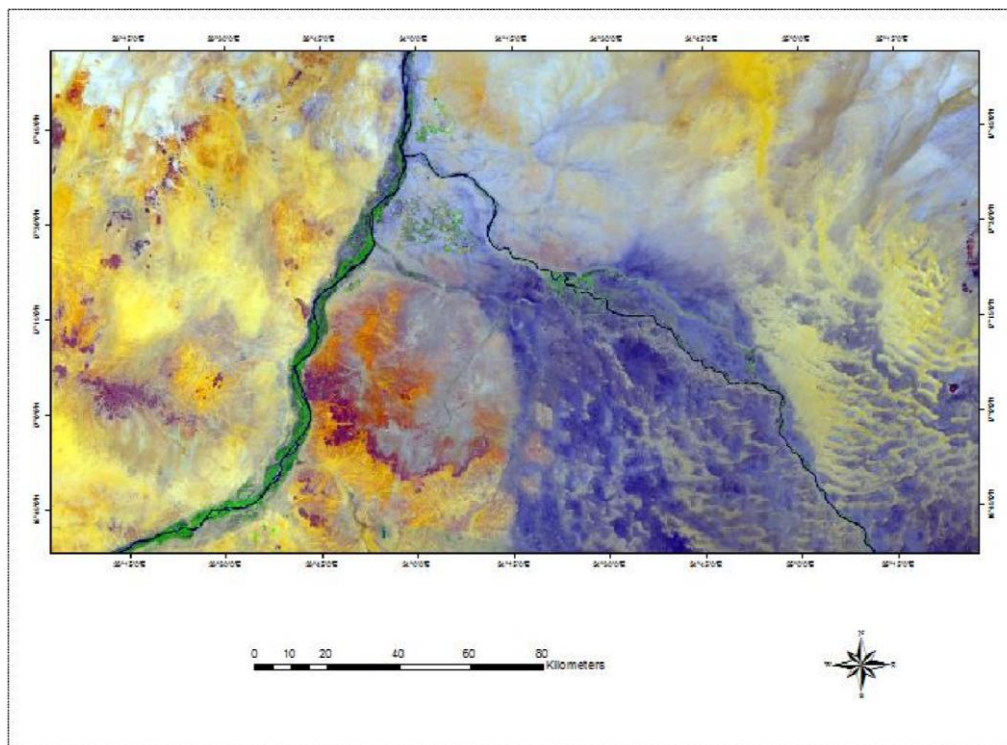


Fig (4.2) Landsat 8 color composite obtained using bands 7, 6 and 1 in RGB respectively

4.1.1.1 Principle Component Analysis (PCA)

Principal component analysis often called PCA, Principal component analysis is a multi-variate statistical technique commonly used in a digital image processing of remotely sensed data (Singh and Harrison, 1985; Loughlin, 1991). The transformation of the raw data using PCA can result in new principal component images that are more interpretable than the original data (Jensen, 1996). The PCA is used to compress the information content of a number of bands of imagery or to reduce the dimensionality from a number of bands to two or three PCs (Jensen, 1996). It is also used to reduce the redundancy of information in highly correlated image set.

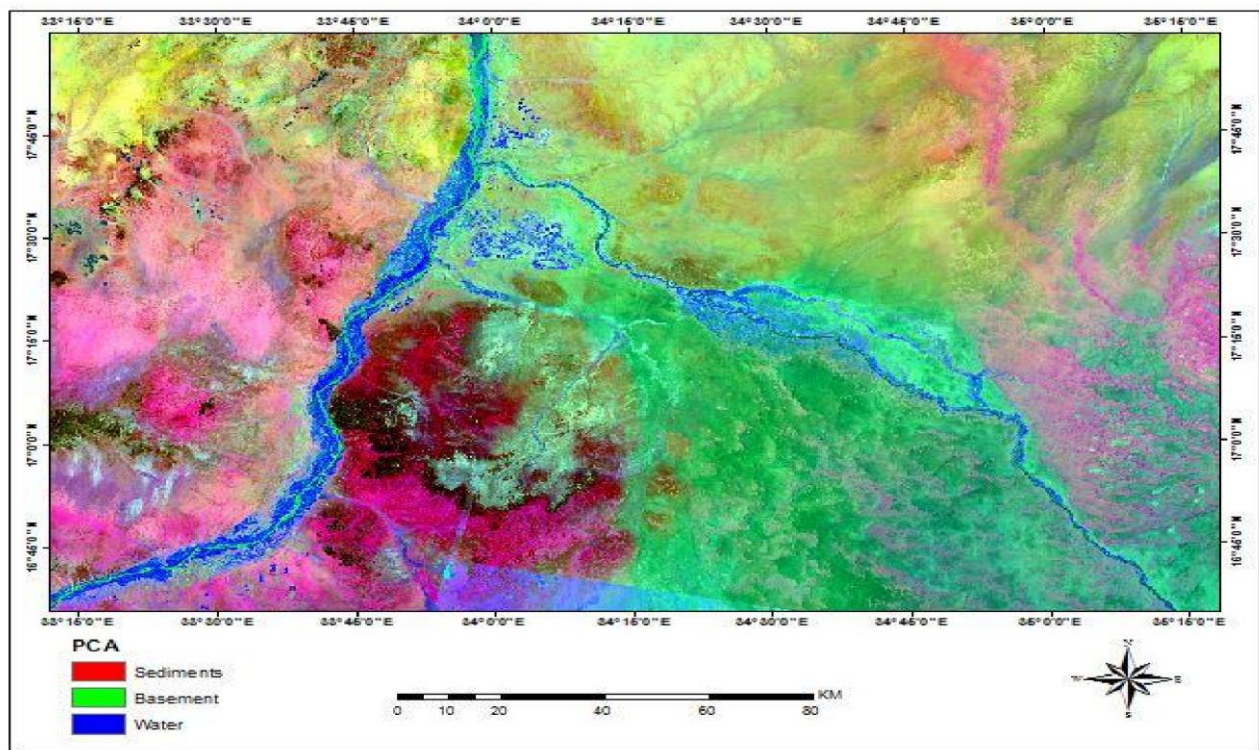


Fig (4.3) Principle Component Analysis (PCA) using PC1, PC2 and PC3 in RGB respectively

4.1.1.2 Extract Lineament Features

Lineaments are simply liner or curvilinear edges that may be related to geological structures, fault, joints, rock composition and line weaknesses. We used satellite image to extract lineaments for different purposes, like defining geological structures and tectonic fabrics Image selection based on visual inspection according to the ability of that image to identify linear and/or curvilinear features. The input data is Landsat subset image with spatial resolution 15m and the output are lineament map and lineaments length. All the image bands were inserted on Geomatica, which showed the lineaments for each band, and then Band 2, 3 and 5 were selected because they contained the most obvious parameters. These lineaments were attached to the laces on Arcgis to give a clear detailing of the shape and length of the lineaments. Analysis and interpretation of the extracted lineaments provided information about the tectonic evolution of the investigated of study area.

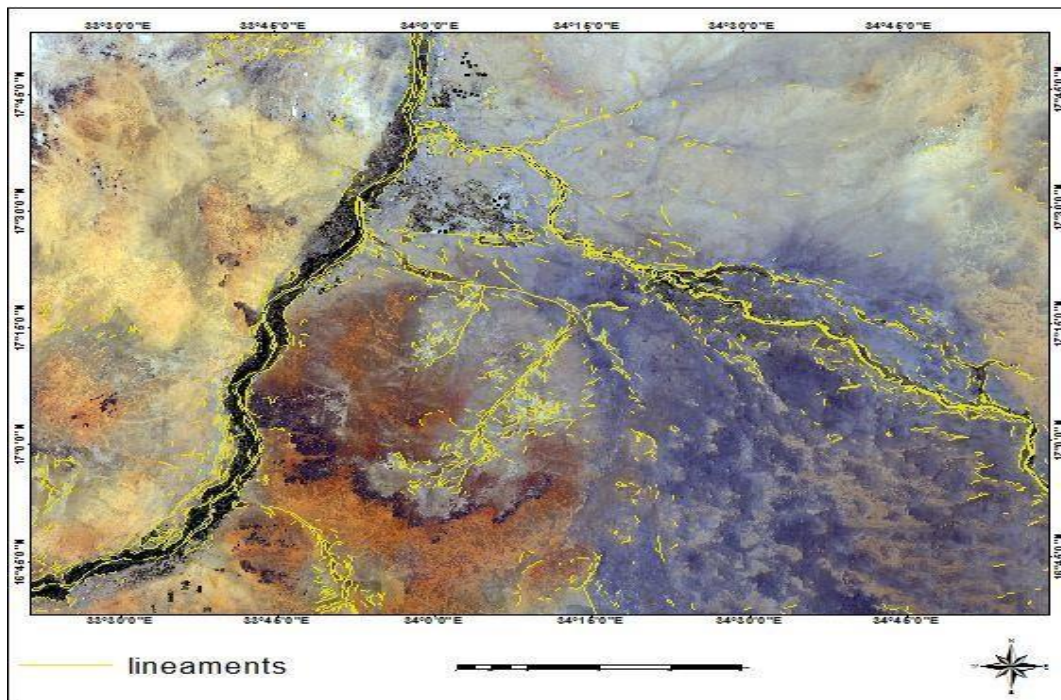


Fig (4.3) Extracted lineaments of the study area.

4.2 Gravity

4.2.1 Introduction

The gravity data of Atbara basin was obtained from the Satellite Geodesy at the Scripps Institution of Oceanography, University of California San Diego. These data were compiled to produce a Bouguer anomaly map, residual anomaly map, first vertical derivatives maps, and first horizontal derivatives maps.

4.2.2 Bouguer Anomaly

Satellite gravity data in the form of Free Air Anomaly (FAA) together with elevation data for each point from 13923 point. These data are processed to calculate the Bouguer correction and hence the Bouguer Anomaly for each point. The results of computations are imported into the GIS environment to interpolate surface between these anomalies, which finally resulted in Bouguer anomaly map with a contour interval of 7mGal for the study area (Fig4.4).

$$\mathbf{BA = FAA - BC} \quad (4_1)$$

$$\mathbf{BC = 0.11195 * Elevation} \quad (4 - 2)$$

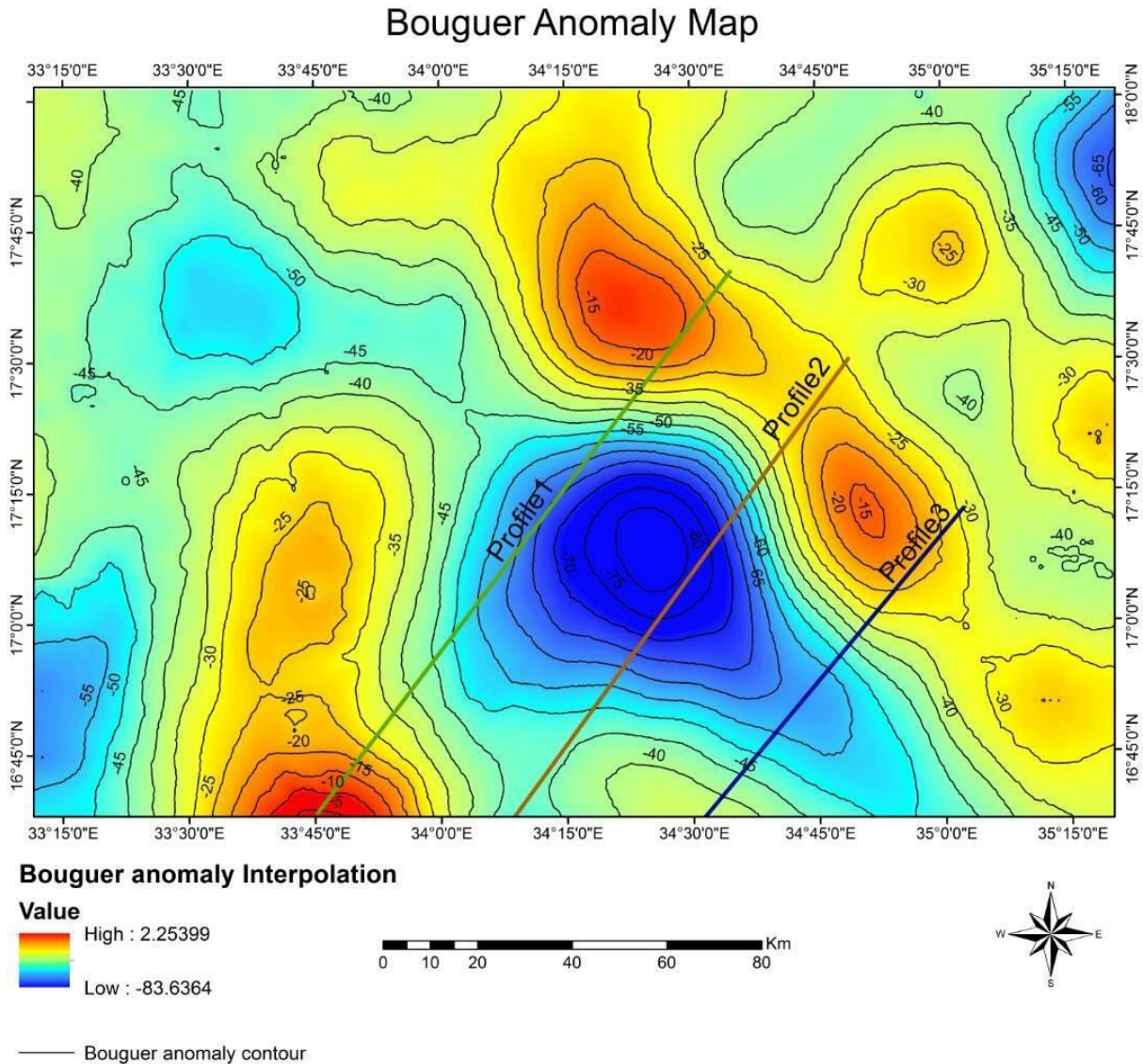


Fig (4.4) Bouguer anomaly map of the study area

4.2.3 Qualitative Interpretation of Bouguer Map

The qualitative interpretation involves the description of the resulting anomaly of gravity data, and the explanation of the major features revealed by these data in terms of types of likely geological formations and Structures. The main feature of Bouguer anomalies over the coastal plain see Fig (4.4) may be summarized as follows:

The Bouguer anomaly map presents many closures around gravity ‘highs’ and ‘lows’. Some of the Bouguer anomalies do not appear to have been caused by surface geology. The regional gravity gradient is increasing in the northeastern and south-west parts and along north-south and north-west directions. The maximum value in the southwestern part of the study area reaches (>2 mGal).

The Bouguer gravity high indicates relatively high density rocks which can be interpreted to indicate basement rocks and the lows to Cretaceous sediments

4.2.4 Qualitative interpretation

4.2.4.1 Regional – Residual Separation

Two types of problems are often encountered in gravity interpretation where anomalies must be separated from one another. The most usual one is where the lateral extent of one anomaly is much greater than the other. This generally occurs when the source with the larger dimensions is a regional geologic feature, such as a basin or geo-synclines, and the smaller one is a local feature, such as an anticline or salt dome. In such a situation. The most common objective in such cases is to isolate the anomaly from the smaller source, a process that involves high pass spatial filtering. The component of the gravity anomaly having the longer effective wavelength is usually referred to as the regional, while the narrower, or shorterwavelength, component having a more localized source is referred to as the residual. Extraction of residual from regional is done both by graphical and computational methods. In regional studies, it may be desirable to remove anomalies from features of small lateral extent so as to bring out larger-scale structures more clearly. Techniques equivalent to low-pass filtering of the observed gravity field should achieve this objective. The widespread use of electronic computers for filtering geophysical data of various kinds has led to the introduction of numerous programs for separating anomalies observed in measuring potential fields such as those from gravity.

In this study we used Polynomial Fitting method obtain the residual anomaly.

$$\text{Residual gravity} = \text{Observed gravity} - \text{Regional gravity}$$

4.2.4.1.1 Polynomial Fitting method:

One of the most flexible of the analytical techniques for determining regional gravity is polynomial fitting. Here the observed data are used to compute, usually by least squares, the mathematically describable surface giving the closest fit to the gravity field that can be obtained within a specified degree of detail. This surface is considered to be the regional gravity, and the residual is the difference between the gravity field as actually mapped and the regional field thus determined.

In practice the surface is expressed mathematically as a two-dimensional polynomial of an order that depends on the complexity of the regional geology. If the regional field were a simple inclined plane, it would be a first-order surface of the form

$$\mathbf{Z} = \mathbf{A}_x + \mathbf{B}_y + \quad (4 - 3)$$

The coefficients A, B, and C are determined so as to minimize the variation of the residual. Agocs2' provides a description of this technique. The next stage of complexity would involve representation by a secondorder polynomial $\mathbf{z} = \mathbf{A}\mathbf{x}^2 + \mathbf{B}\mathbf{y}^2 + \mathbf{C}_{xy} + \mathbf{D}_x + \mathbf{E}_y + \mathbf{F}$ (4 - 4)

Polynomials of much higher order would probably be necessary for a large area over which the regional has numerous convolutions. The approach is quite similar to that used in trend-surface analysis, a technique that has seen increasing use in reconstructing geologic structures as they should have appeared before regional deformation took place.

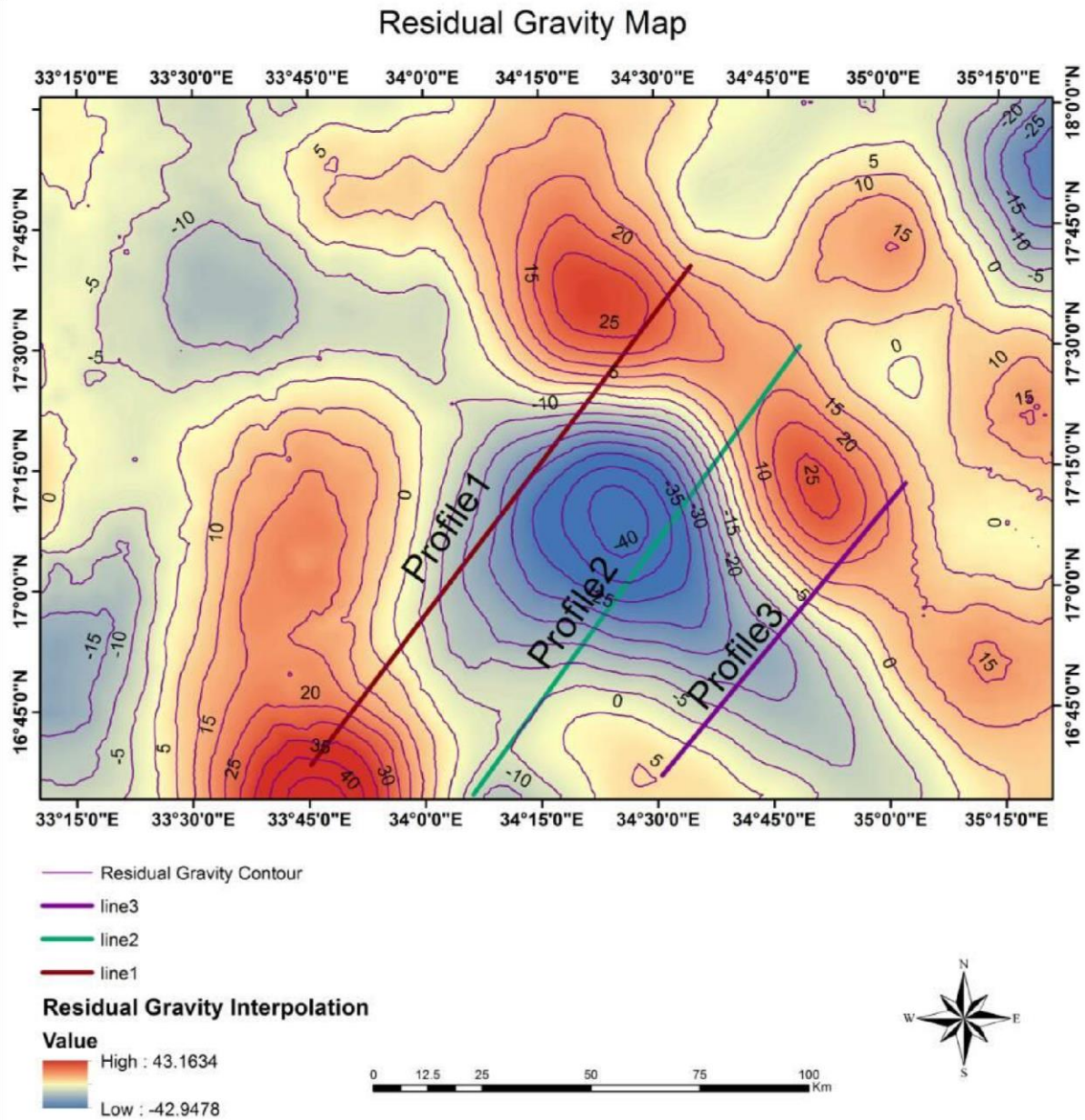


Fig (4.5) Residual gravity map of study area

4.2.5 First Vertical derivative

First-vertical-derivative maps can serve many of the same purposes as second-vertical-derivative maps, and the noise amplification problem is not quite as severe. Moreover, a physical significance can be attached to the first vertical derivative.

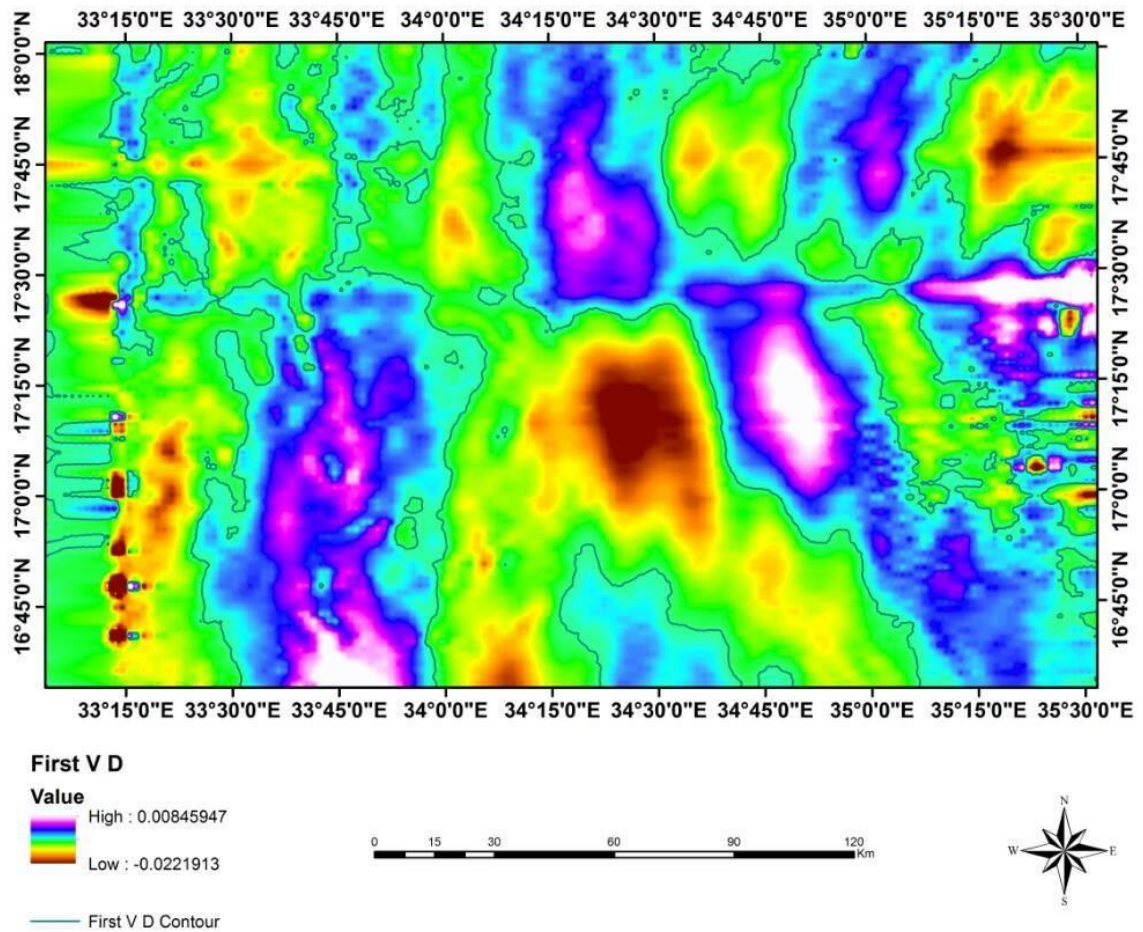


Fig (4.6) First Vertical Derivative Map

4.2.6 First Horizontal Derivative

The first horizontal derivative may be qualitatively interpreted by considering the Zones of maximum gradients for determining probable fault system and /or lithological contacts. Which are present in the area. In figure (4.7) shows, contains a linear maximum gradient trending NW and NE. In the northern part of the first horizontal derivative map there are three linear patterns of dense contours oriented in a NE and NW direction. The extension of maximum horizontal gradient zones and their orientation are utilized to determine faults extension and their orientations respectively.

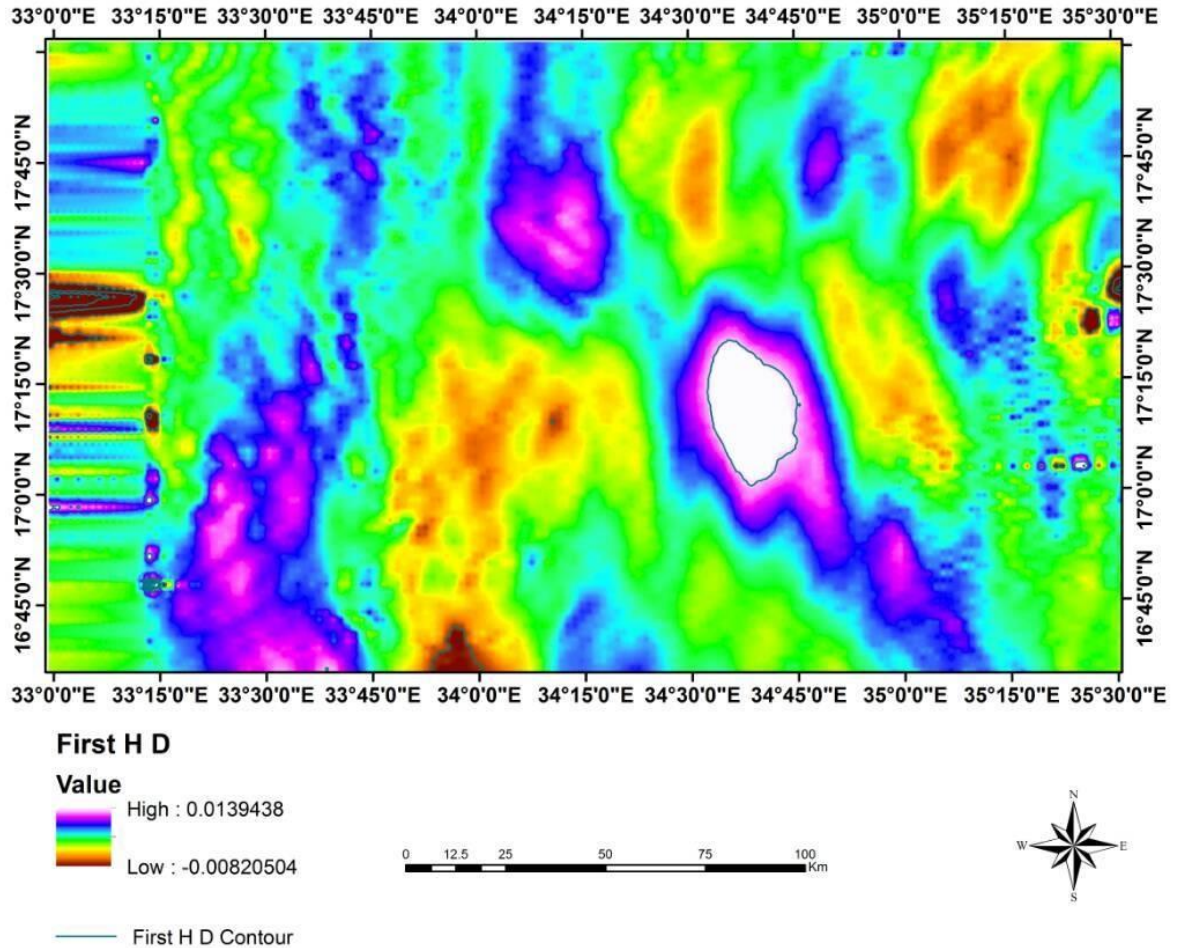


Fig (4.7) First Horizontal Derivative Map

4.2.7 2D Modeling

Quantitative Interpretation (non-linear method) calls for approximation of the geological bodies, which are considered to be the gravity source, by assuming simple geometric model from which the theoretical gravity effect can be compared with the observed gravity data and the shape of the body can be changed (modified) to minimize the difference between the observed and the computed gravity effects, often by interactive and/or iterative computer inversion methods (Kearey and Brooks, 1988).

The modeling technique calls for approximation of the geological feature considered being the source by assigning it a simple geometrical form for which the gravity field can be computed mathematically by specified dimension and various values can be assigned to the parameters describing the geometry of these bodies. Modeling of the anomalies. In this study was performed by using slab formula. Three profiles has been created in the study area in NE-SW direction cross the low gravity anomalies.

4.2.8. Density Measurements

The interpreter of the gravity data is interested in determining the subsurface variations of mass and this process requires that the density of the material of interest or the density contrast between the surrounding materials be known. For this reason especial attention is paid to the densities and the density contrasts between different representative rock types in the surveyed area. The average density measurements for all the sedimentary formations (2.3 g/ cm³) and the Basement rocks of the area (2.68 g/ cm³). So the density contrast is (-0.38 g/cm³).

4.2.9 Result and Discussion

Profile 1

The profile runs in the NW-SE (Fig 4.8). The gravity field along the profile represents paired Bouguer gravity anomaly with low gravity anomaly in the center and eastern part of the model flanked by two highs of different amplitudes (Fig.45). The first derivative of these profiles defines two normal faults (Graben). The maximum depth obtained by models is about 1500 m.

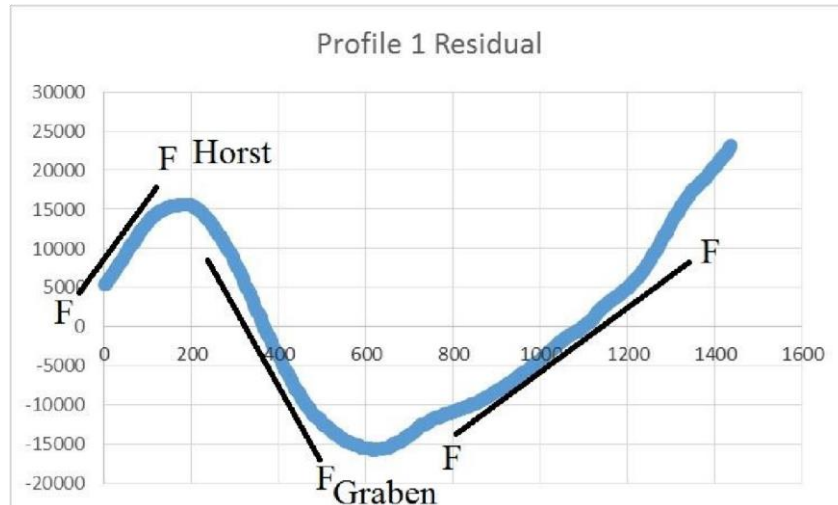


Fig (4.8) Gravity model of profile (1).

Profile 2

The profile runs in the NW-SE (Fig 4.9). The gravity field along the profile represents paired Bouguer gravity anomaly with low gravity anomaly in the center and eastern part of the model flanked by two highs of different amplitudes (Fig.45). The first derivative of these profiles defines two normal faults (Graben). The maximum depth obtained by models is about 2500 m.

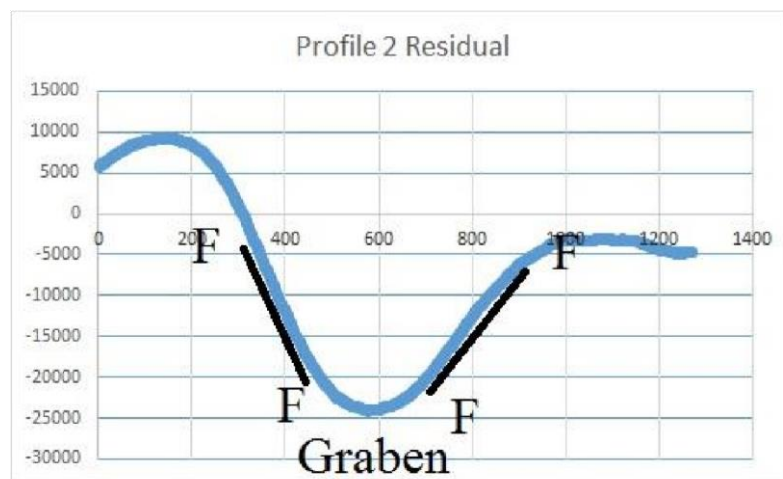


Fig (4.9) Gravity model of profile (2).

Profile 3

The profile runs in the NW-SE (Fig 4.10). The gravity field along the profile represents paired Bouguer gravity anomaly with low gravity anomaly in the center and eastern part of the model flanked by two highs of different amplitudes (Fig.45). The first derivative of these profiles defines two normal faults (Graben). The maximum depth obtained by models is about 2500 m.

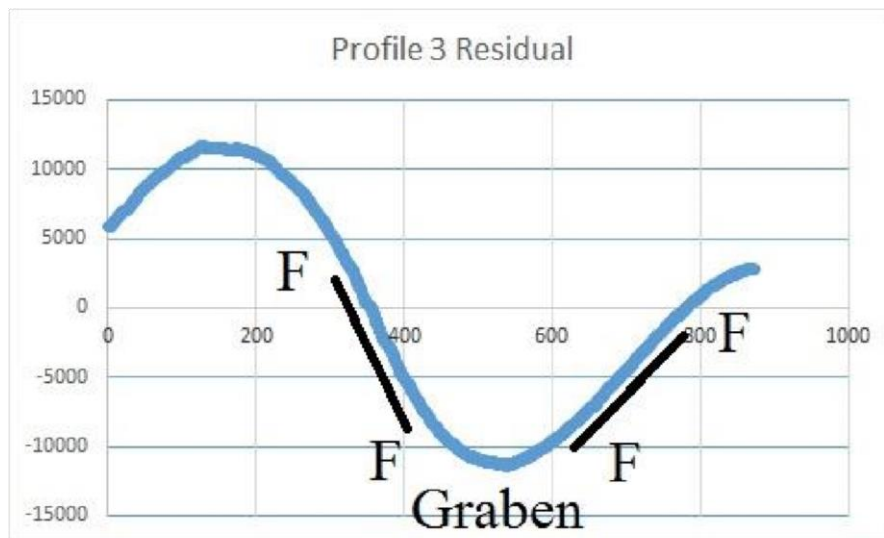


Fig (4.10) Gravity model of profile (3).

Chapter Five

Conclusions

Atbara Basin is the large basins compare to other central Sudan basins. This study has found that the basin appears to be divided into sub-basins separated by structural.

The basin does not extend very far to the NW. To the SE, the basin gradually gets shallower so the boundary is unclear. The central basin in profile 2 is the deepest and largest of the basin and lies adjacent to the main Atbara fault which defines the NE-NW boundary of the basin

The results were obtained from this study was constrain with AlKandaka Well, the output was acceptable and satisfied.

The method is free and powerful, we recommended to apply it in rest of areas in Sudan not covered by gravity or have lack of data. And this will lead to discover new basin and develop to understand the tectonic setting of Sudan.

References

- **Ahmed and Badi (2008):** Conducted research to detect the bacteriological pollution of groundwater in Shendi-Atbara Basin, River Nile State, Sudan.
 - **Bussert (1993):** Studied the intracratonic basins evolution in the central northern Sudan showing the contrast with typical cratonic sandstone sheets of North Africa.
- **Cox, L. R. (1932),** On Fossiliferous Siliceous boulders from the AngloEgyptian Sudan *proc.geol.Lndon.*
- **GREENWOOD A. G. (1976).** Recent advances in clinical and diagnostic techniques in marine mammals. European Association for Aquatic Mammals, 4th Annual Symposium, Mallorca, Spain.
- **Jensen** digital image processing : remote sensing perspective.
 - **Jorgensen and Bosworth (1989):** Made gravity modeling in the Central African Rift System, Sudan, and identified rift geometries and tectonic significance.
 - **KARKANIS (1945)** Stratigraphical. Notes, AngloEgyptian Sudan. Sudan Notes and Records.
- **Kheiralla, M. K., 1966:** A study of the Nubian Sandstone Formation of the Nile between 140 N and 170 42N.
- **Loughlin, W. P., (1991),** Principal component analyses for alteration mapping. *Photogrammetric Engineering and Remote Sensing.*
- **Milton B.Dobrin and Carl H. Savit (1976),** Introduction to geophysical processing .
- **Mohammed S. A. Abdalla and Kamal F. Elkhaliifa (2010):** Tree and Shrub Species at Lower Atbara River Basin, Northeastern Sudan.

- **Mohammied Zayed Awad (2015):** PetroLeum GeoLogy and Resources of the Sudan.
- **Omer (2013):** Studied groundwater sources, geological formations, and their environment in Sudan.
- **Robert schowengerdt, (2007)** remote sensing: models and methods for image processing.
- **Russegger J.R. (1837)** Kreide und Sandstein einfluss von Granit auf Ietzteren [Chalk and sandstone: the influence of granite on the Latter].
- **Singh, A., and Harrison, A., (1985),** Standardized principal components, International Journal of Remote Sensing.
- **Salama (1997):**Studied the Sudanese intracratonic rift basins on the basis of geophysicalsurvey, delineating NW-SE trending Cretaceous sediment troughs and mentioned thatwadi El Mukabrab in the northern part of the study area represents a fault boundary.
- **VaiI, J. R. (1979),** Outline of geology and mineralization of the Nubin Shield east of the Nile Valley, Sudan. - In: TAHON. S. A. (ed). Evolution and mineralization of the Arabian Nubian Shield.